NUMERICALLY EFFICIENT NONLINEAR DYNAMIC ANALYSIS OF BARGE IMPACTS ON BRIDGE PIERS

By

DAVID RONALD GAYLORD-COWAN

A THESIS PRESENTED TO THE GRADUATE SCHOOL
OF THE UNIVERSITY OF FLORIDA IN PARTIAL FULFILLMENT
OF THE REQUIREMENTS FOR THE DEGREE OF
MASTER OF ENGINEERING

UNIVERSITY OF FLORIDA

2004

ACKNOWLEDGMENTS

Completion of this thesis and the research associated with it would not have been successful without the help and guidance of a number of individuals. First and foremost, the author would like to thank Dr. Gary Consolazio. His support in this endeavor has proved most valuable, and without it, the author would not have been able complete the research presented herein. He provided invaluable knowledge and insight that the author will carry with him through all future undertakings.

The author also wishes to thank Dr. Ronald Cook for his contributions to experimental research done in conjunction with this research, Dr. H.R. (Trey) Hamilton for his valuable insights on design for related research, and Dr. Mark Williams for his assistance with FB-Pier. Others deserving of thanks for their support and contributions include Alex Biggs, Jessica Hendrix, Ben Lehr, and Bibo Zhang.

The author wishes to thank his friends and family for their support and encouragement.

TABLE OF CONTENTS

LIST OF FIGURES

Abstract of Thesis Presented to the Graduate School
of the University of Florida in Partial Fulfillment of the
Requirements for the Degree of Master of Engineering

NUMERICALLY EFFICIENT NONLINEAR DYNAMIC ANALYSIS OF BARGE IMPACTS ON BRIDGE PIERS

By

David Ronald Gaylord-Cowan

December 2004

Chair: Gary R. Consolazio
Cochair: Ronald A. Cook
Major Department: Civil and Coastal Engineering

Designing bridge structures that cross navigable waterways requires attention be given to vessel impact scenarios. Currently, design specifications account for vessel impact through the use of empirical equations that yield an equivalent static load. In this thesis, focus is placed on using dynamic analyses of vessel impact—specifically barge impact—to design bridge structures. Using the LS-DYNA finite element code, force-deformation relationships are developed for several barge crushing scenarios. With these force-deformation relationships as input and a numerically efficient dynamic time-stepping algorithm, nonlinear barge and pier analyses can be conducted in relatively short periods of time. In particular, focus has been given to the development of algorithms capable of modeling cyclic loading of barge bows and oblique angle impacts. Several case studies are conducted by varying the following input parameters: pier stiffness and shape, impact speed and angle, and barge mass. For demonstration, the method presented

herein is implemented in an existing bridge substructure analysis program to validate its accuracy and to conduct the previously mentioned case studies.

CHAPTER 1
INTRODUCTION

Designing bridges that span navigable waterways requires the designer to compute loads due to vessel impact. When a vessel—such as a barge or ship—impacts a supporting pier of a bridge (the most common impact scenario), the result is a substantial lateral force. This force is transmitted to both the foundation and bridge deck—influencing the soil and other piers supporting the bridge. Due to the large mass associated with vessels and their cargo, impact type loading is fundamentally dynamic in nature. Thus, the load imparted to the structure will vary with respect to time. Magnitude, duration, and periodicity of the load history are affected by the structural configuration, mass, and velocity of the barge; the mass and stiffness of the pier; and the type of soil.

Impacts involving barges occur more frequently than impacts involving ships [1]. A major reason for this phenomenon is that most bridges that span over water, span over inland waterways. Many of these waterways—due to limited water depth—can only be traversed by shallow draft vessels, such as barges, whereas deeper draft vessels, such as ships, are limited to traversing deep bodies of water. As such, barge impact loading was selected as the main topic of this research. However, the concepts presented in this paper are easily extrapolated to research involving ship impacts.

A variety of experimental and analytical vessel collision tests—on both barges and ships—have been conducted and reported in the literature. Forming the basis for the AASHTO (American Association of State and Highway Transportation Officials) barge

provisions, Mier-Dornberg [2] researched loading—both static and dynamic—on scale barge models. Arroyo et al. [3] conducted full-scale barge flotilla impact tests on lock walls and used the results to generate a method that correlates maximum impact force to linear momentum. Jagannathan and Gray [4] developed an analytical model for barge impacts on rigid structures and compared results to a time-domain analysis.

Minorsky [5] conducted analyses on ship collisions—with reference to protection of nuclear powered ships—to analyze the extent of vessel damage. Woisin [6] also analyzed nuclear powered ship collisions by conducting experiments on scale models. Furthermore, Woisin's results were used in the development of AASHTO's ship design provisions [7]. Using a finite element approach, Kitamura [8] investigated the effects of collisions between ships, and compared the results to simplified analytical methods. Lehmann and Peschmann [9] conducted large-scale ship collision tests and compared the test results to results from finite element analyses. Chen [10] provided an efficient simplified model of ship collision damage prediction that can be used in probabilistic analyses. Using a derived analytical method, Frieze and Smedley [11] investigated many scenarios that involve ship collisions.

Although barge impact loading is of a dynamic nature, current bridge design procedures for impact loading provide simplified procedures for determining static equivalent loads intended to produce a similar response as a dynamic load history. In the U.S., procedures for determining equivalent static loads for barge impact events are provided by the AASHTO bridge design specifications [7]. Equations relating barge kinetic energy to barge deformation—referred to as crush depth—and then crush depth to an equivalent static load are included in the AASHTO barge impact provisions.

Another option for designing for barge impact loading requires the designer to develop high resolution finite element models for use in conducting dynamic impact simulations. This process can be extremely time consuming and thus does not lend itself to use in a design office. Barge and pier models can take months to create, refine, and validate; and individual impact simulations can take days to complete.

In this thesis, the development and testing of a numerically efficient analytical method for determining loads imparted to a pier during a barge impact scenario is presented. Unlike the AASHTO specifications, this method computes a dynamic load history and pier response without requiring use of high-resolution dynamic finite element analyses. This method can be implemented in existing design-oriented analysis software which is capable of dynamically analyzing pier response under varying barge impact loading conditions. Factors such as barge mass, impact speed, impact angle, pier stiffness, pier mass, pier geometry, and soil conditions may all be taken into consideration.

One key component of the proposed method is the force-deformation relationship for the barge head log, which can be obtained by either full-scale barge experiments or high-resolution static finite element analysis. The latter method was chosen for the research presented here.

Before discussing specific analytical methods used for creating such force-deformation relationships (Chapter 3), a brief review of the AASHTO equivalent static force calculation procedures is presented (Chapter 2). Later, details of the proposed impact analysis algorithm are presented (Chapter 4) and the method is demonstrated

using several case studies (Chapter 5). Finally, conclusions and recommendations are offered (Chapter 6).

CHAPTER 2
AASHTO METHOD FOR PREDICTION OF BARGE IMPACT LOADS

Barge impact load calculations conducted according to the AASHTO provisions involve the use of both an empirical load prediction model and a risk assessment procedure. The AASHTO guide specification for vessel collision design [7] and the AASHTO LRFD bridge design specifications [12] differ in the risk assessment methods available in each document (Ref. [12] provides only a subset of the options available in Ref. [7]). However, the load prediction model implemented, which is the item of interest here, is the same in both of these documents.

AASHTO-based load calculations for barge impact design begin with selection of the "design" impact condition (barge type and impact speed). Factors such as the characteristics of the waterway, expected types of barge traffic, and the importance of the bridge (critical or regular) enter in to this selection process. Once the impact conditions have been identified, the kinetic energy of the barge is computed as [7]

$$KE = \frac{C_H W V^2}{29.2} \tag{2.1}$$

where KE is the barge kinetic energy (kip-ft), C_H is the hydrodynamic mass coefficient (a factor that approximates the influence of water surrounding the moving vessel), W is the vessel weight (in tonnes where 1 tonne = 2205 lbs.), and V is the impact speed (ft/sec). It is noted that Eq. 2.1 is simply an empirical version (derived for a specific set of units) of the more common relationship

$$KE = C_H \left(\tfrac{1}{2} M V^2 \right) \tag{2.2}$$

where KE, M (the vessel mass), and V are all dimensionally consistent.

Once the kinetic energy of the barge has been determined, a two-part empirical load prediction model is used to determine the static-equivalent impact load. The first component of the model consists of an empirical relationship that predicts crush deformation as a function of kinetic energy

$$a_B = \left(\sqrt{1 + \frac{KE}{5672}} - 1 \right) \cdot \left(\frac{10.2}{R_B} \right) \tag{2.3}$$

In this expression, a_B is the depth (ft.) of barge crush deformation (depth of penetration of the bridge pier into the bow of the barge), KE is the barge kinetic energy (kip-ft), and $R_B = \left(B_B / 35 \right)$ where B_B is the width of the barge (ft).

The second component of the load prediction model consists of an empirical barge-crush model that predicts impact loads as a function of crush depth

$$P_B = \begin{cases} 4112\, a_B\, R_B & a_B < 0.34 \text{ ft.} \\ \left(1349 + 110\, a_B \right) R_B & a_B \geq 0.34 \text{ ft} \end{cases} \tag{2.4}$$

where P_B is the equivalent static barge impact load (kips) and a_B is the barge crush depth (ft). The crush model represented by Eq. 2.4 is illustrated graphically in Figure 2.1.

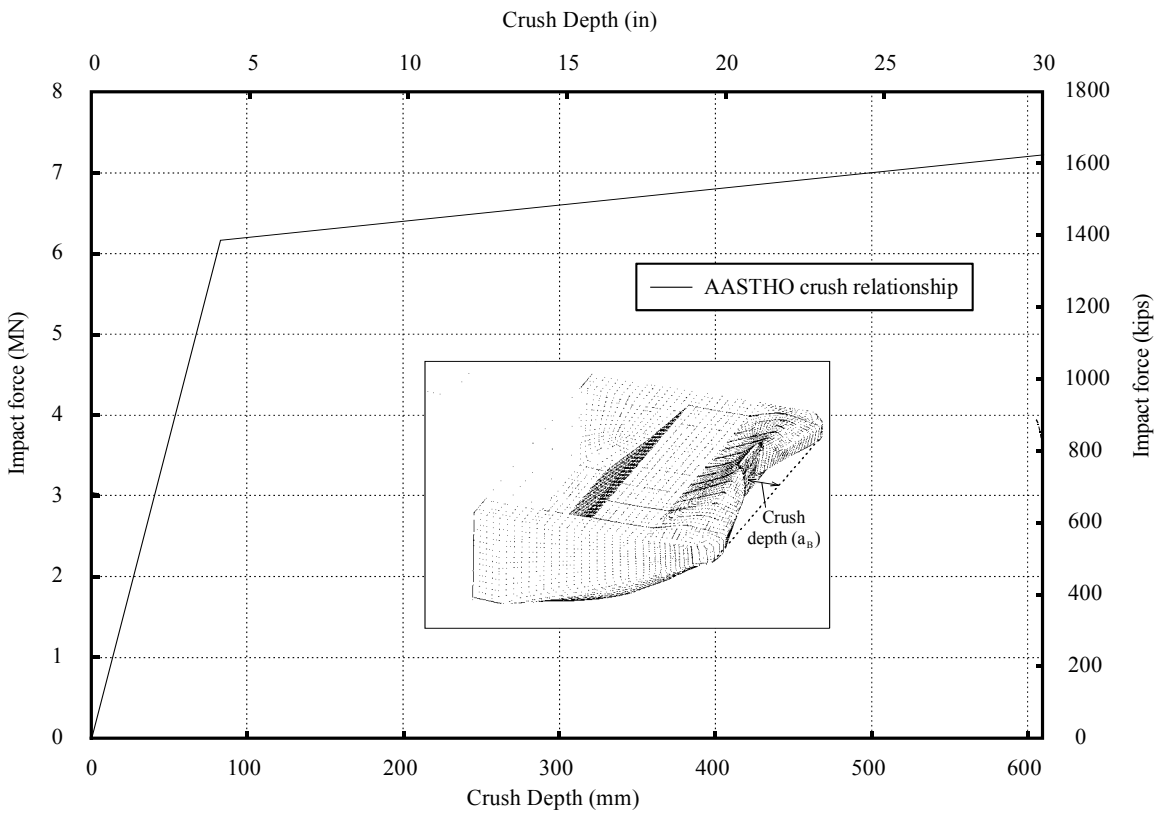

Figure 2.1 Barge crush model used in AASHTO bridge design specifications

Unfortunately, since very little barge collision data hve ever been published in the literature, Eqs. 2.3 and 2.4 are based on a single experimental study. During the early 1980s, a study was conducted in Germany by Meir-Dornberg [2] that involved physical testing of *reduced-scale* standard European (type IIa) barges. Experimental barge crush data were collected by Meir-Dornberg and then used to develop empirical relationships relating kinetic energy, depth of barge crush deformation, and impact load. AASHTO's relationships, Eqs. 2.3 and 2.4, are virtually identical to those developed by Meir-Dornberg except that a width-modification factor—the R_B term—has been added to approximately account for deviations in barge width from the baseline width of 35 ft. (the width of barges most often found operating in U.S. inland waterways).

Interestingly, while Eq. 2.3 utilizes the R_B term to reflect the influence of barge width, no such factor has been included to account for variations in either the size (width) or geometric shape of the bridge pier being impacted. Furthermore, since Eq. 2.4 indicates that the impact load (P_B) increases monotonically with respect to crush depth (a_B), the AASHTO provisions implicitly assume that maximum impact force occurs at maximum crush depth, and therefore, peak impact load can be uniquely correlated to peak crush depth. In the following chapter, finite element simulations will be used to demonstrate that this assumption does not always hold true.

CHAPTER 3
FINITE ELEMENT COMPUTATION OF BARGE FORCE-DEFORMATION RELATIONSHIPS

3.1 Introduction

A key aspect of the efficient barge impact analysis method developed in this thesis involves the use of precomputed barge force-deformation crush relationships. Analysis of structural crushing is very often handled using nonlinear contact finite element simulation. In the case of vessel crush simulation, the finite element code used must be capable of robustly representing nonlinear inelastic material behavior (with failure), part-to-part contact, self-contact, and large displacements (due to the significant geometric changes that often occur). The LS-DYNA finite element code [13] meets all of these requirements and has been shown in previous studies to be capable of accurately simulating complex structural crushing. LS-DYNA was thus employed throughout the present investigation to study crushing of barges.

The high-resolution barge model used in the current study was previously developed based on detailed structural plans of a jumbo class hopper barge. Details including steel material properties, finite element types, etc. used for the barge model are documented in existing literature [14-16].

3.2 Pier Impactor Models and Crush Conditions

Of particular interest in this study is the crush behavior that occurs when barges collide with concrete bridge piers. As such, the geometric shapes of the impactors developed herein match the two most common bridge pier shapes—circular and square.

Each impactor is modeled using eight-node solid elements, is assigned a nearly-rigid linear elastic material model, and is positioned along the longitudinal axis of the barge (Figure 3.1) at a location that initially produces a small gap between the surfaces of the barge and the pier impactor. A contact definition is then defined between these surfaces with a friction value of $\mu = 0.3$ (approximate frictional coefficient for steel sliding on concrete). Nodes on the back face of the impactor (opposite the contact surface) are then assigned a displacement time history that translates the pier toward the barge at a constant rate of 10 in/sec to generate crushing of the barge bow. At each time step in this analysis procedure, the contact force acting between the pier face and the barge bow is computed along with the corresponding crush deformation (penetration) that has occurred at that point in time. The relationship between force and deformation thus obtained may then be used as a vessel crush curve in other analysis procedures.

3.3 Discussion of Static Crush Simulation Results

Static barge crush analyses are conducted for five circular pier diameters: 0.610 m, 1.219 m, 1.829 m, 2.438 m, 3.048 m (2 ft, 4 ft, 6 ft, 8 ft, 10 ft) and five square widths: 0.610 m, 1.219 m, 1.829 m, 2.438 m, 3.048 m (2 ft, 4 ft, 6 ft, 8 ft, 10 ft). For each level of imposed penetration, i.e. barge crush depth, the total force acting at the contact interface between the pier and the barge is extracted from the finite element simulation data. Results obtained from the circular crush simulations are presented in Figure 3.2. Forces acting on the pier (i.e. the impactor) are shown to gradually and monotonically increase with corresponding increases in crush depth. In general, the crush characteristics are also shown to be slightly sensitive to variations in pier width, but the effect is not strongly pronounced.

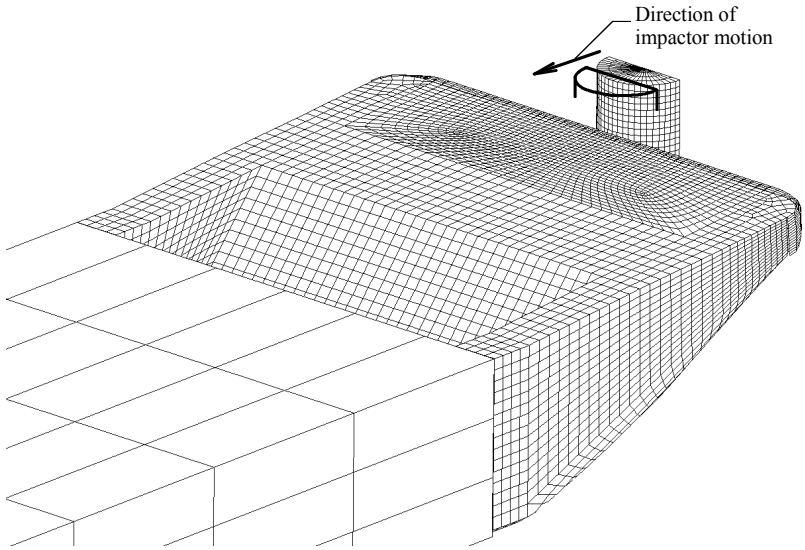

a) Crush model consisting of barge and circular pier impactor

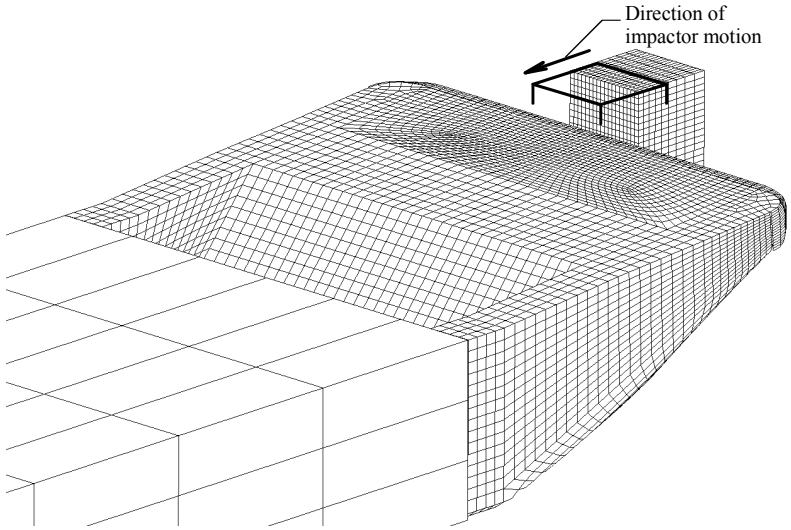

b) Crush model consisting of barge and square pier impactor

Figure 3.1 Crush simulation models

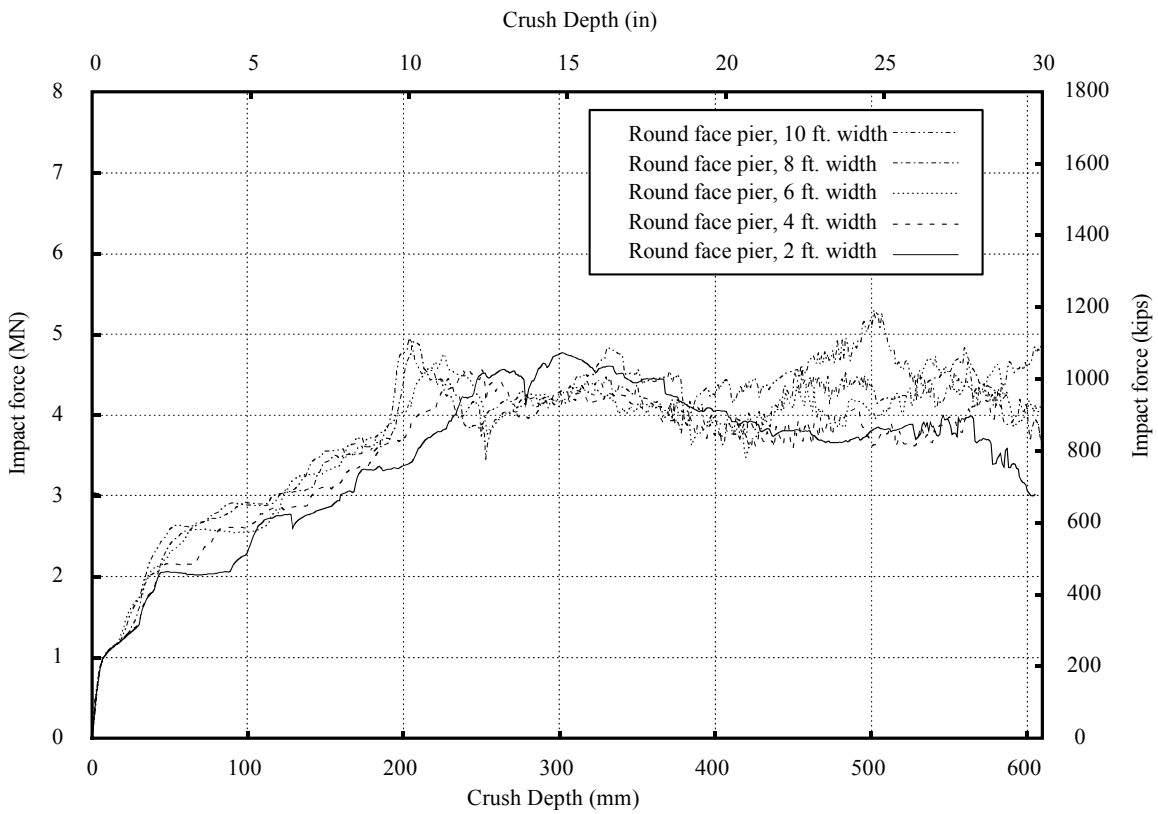

Figure 3.2 Predicted barge crush behavior for circular impactors

In Figure 3.3, crush results are presented for the square impactor simulations. Several key differences between the circular and square crush cases are immediately evident. In the square crush cases, the contact forces are observed to rise very rapidly and—for small deformation levels—the overall crush behavior is seen to be much stiffer than in the circular cases. However, after the contact force has maximized, the stiffness of the barge diminishes rapidly in the square cases. In fact, whereas all of the *circular* crush analyses predicted a monotonically increasing relationship between force and crush depth, *none* of the square analyses exhibited this characteristic. In addition, whereas diameter had very little effect on the crush behavior observed for circular piers, Figure 3.3 indicates that in square crush conditions, there is a definite relationship between pier width and force generated.

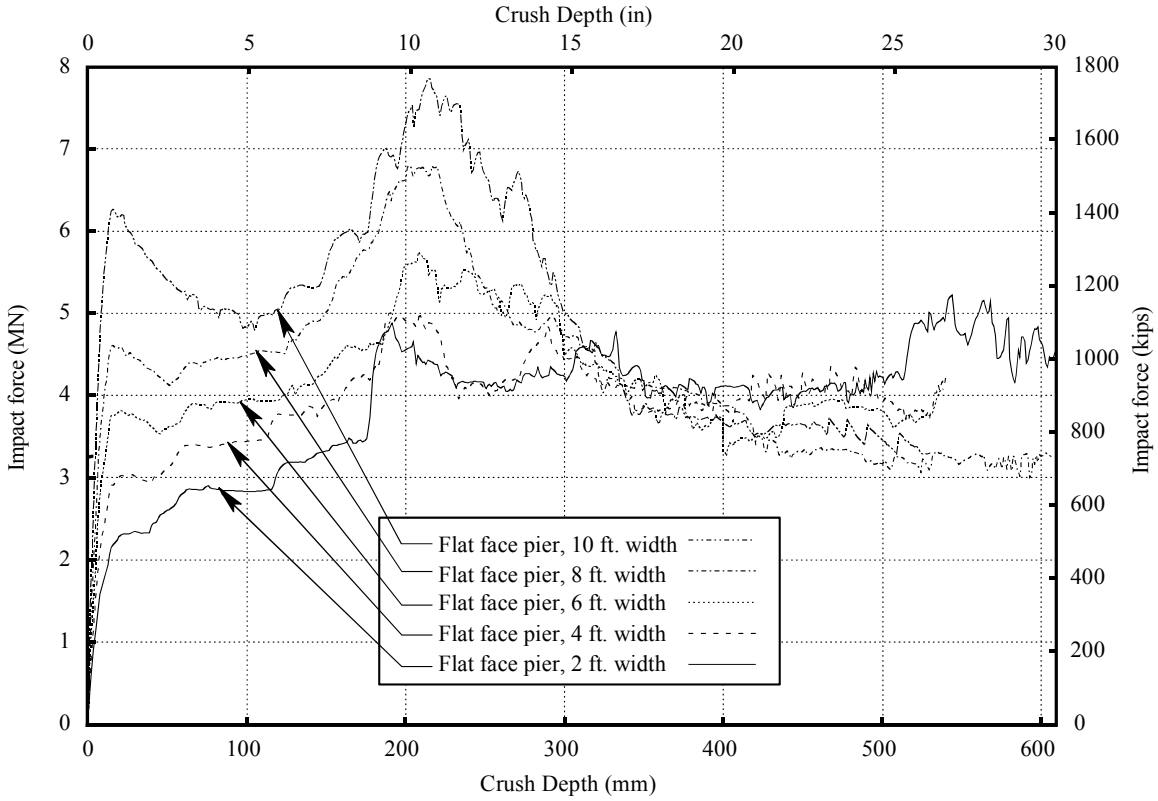

Figure 3.3 Predicted barge crush behavior for square impactors

That pier geometry can influence the crush behavior of a barge is not surprising when consideration is given to the internal structure of such vessels. In the bow of a barge, numerous internal trusses run parallel to one another resulting in significant stiffness in the longitudinal direction. During impact with a pier, both the shape and size of the pier determine the number of internal trusses that actively participate in resisting bow crushing. Figure 3.4 illustrates the internal deformation produced by 12 in. of crush depth imposed by a 6 ft. diameter circular impactor. Figure 3.5 illustrates the same scenario, but for a 6 ft. wide square impactor. In the circular case, bow deformation is concentrated in a narrow zone near the impact point and only the trusses immediately adjacent to this location generate significant resistance. As increasing crush deformation

occurs, additional trusses participate and the force increases in an approximately monotonic manner.

In contrast, when a *flat-surface* square impactor bears against the barge, several trusses immediately and simultaneously resist crushing, thus producing a very stiff response. However, when the trusses buckle, and therefore soften (Figure 3.5), they all do so at approximately the same deformation level. As a result, there is an abrupt decrease in the overall stiffness of the barge (as was illustrated in Figure 3.3 where the crush forces plateau or even decrease after maximizing). After this initial softening, there is an increase in loading to a second peak. It is believed that this second peak is a result of the contribution to the barge resistance of the internal members adjacent to those members inline with the impactor. As these adjacent members buckle and soften, there is a subsequent decrease in loading.

In addition, increasing the width of a square pier increases the number of trusses that simultaneously participate in crushing, thus explaining the sensitivity of force magnitude to impactor width that was evident in the square crush simulations. As was noted earlier, the AASHTO crush model given in Eq. 2.4 includes a correction factor (R_B) for barges that deviate from the 35 ft. width of the standard hopper barge. However, the finite element results presented here suggest that it may also be appropriate to include parameters reflecting the effects of pier shape and pier size in the crush model as well.

A comparison of the empirical AASHTO crush model, Eq. 2.4, and finite element predicted crush is presented in Figure 3.6. For cases involving circular impactors (Figure 3.6a) where the barge head log exhibits significant crush deformation (e.g. more than 6 in.), the forces predicted by finite element simulation are significantly less than those

predicted by the AASHTO crush model. However, for cases involving square impactors (Figure 3.6b) it is important to note that while impactor widths of 2 ft, 4 ft, and 6 ft predict lower forces than the AASHTO methods when there is significant barge crushing, impactor widths of 8 ft and 10 ft predict loads that are high than the AASHTO relationship at a approximate crush depth of 200 mm (10 in).

In addition, impactor data shown in Figure 3.6 demonstrate that, for some pier configurations, the static crush force does not necessarily increase monotonically with respect to crush depth. In such cases the maximum force generated cannot necessarily be correlated to the maximum crush depth sustained (e.g. in an impact condition). This fact is important because the AASHTO load prediction procedure described earlier (Eqs. 2.1, 2.3, and 2.4) assumes that the equivalent static impact force can be uniquely correlated to (or predicted from) peak crush deformation sustained by a barge during an impact event. The square impactor crush results presented here indicate that this procedure should be reexamined since impact force does not appear to be uniquely correlated to maximum deformation.

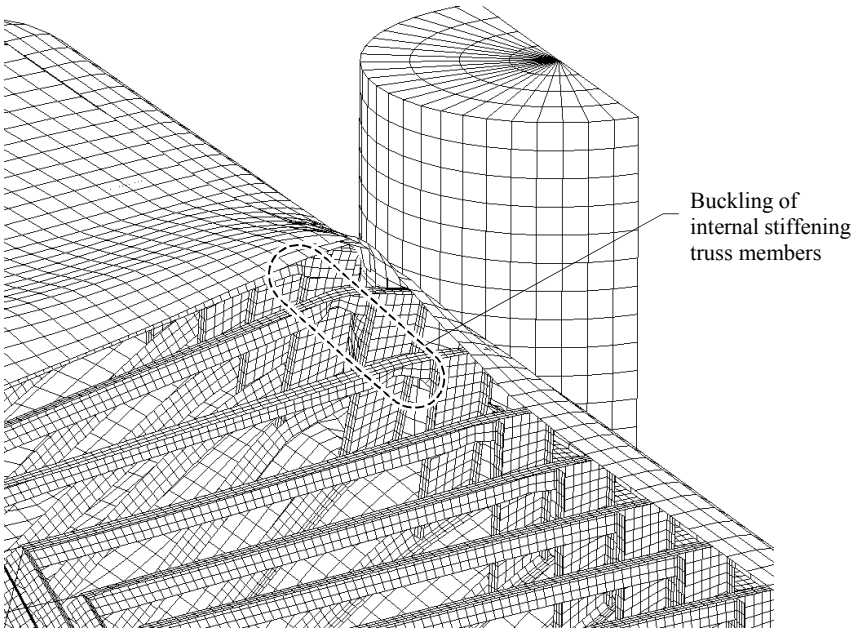

Figure 3.4 Barge deformation generated by circular pier impactor

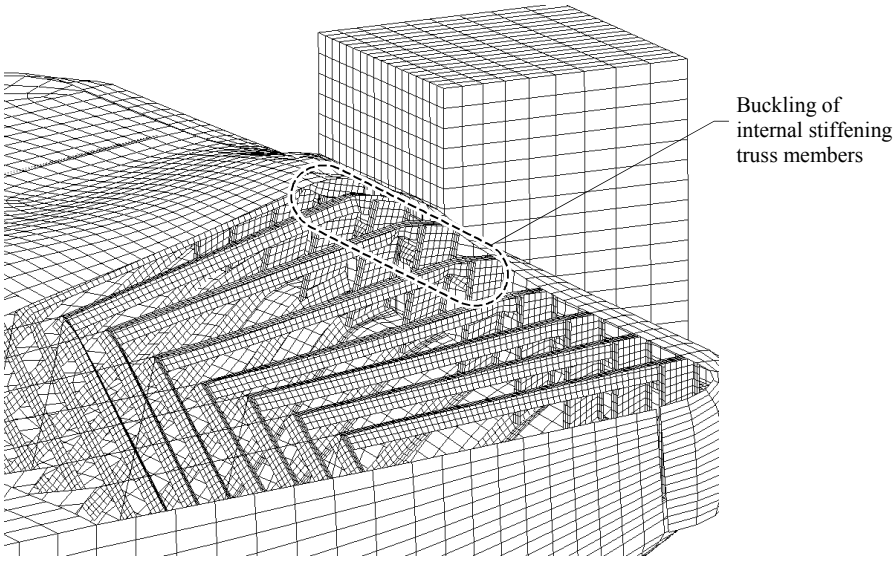

Figure 3.5 Barge deformation generated by square pier impactor

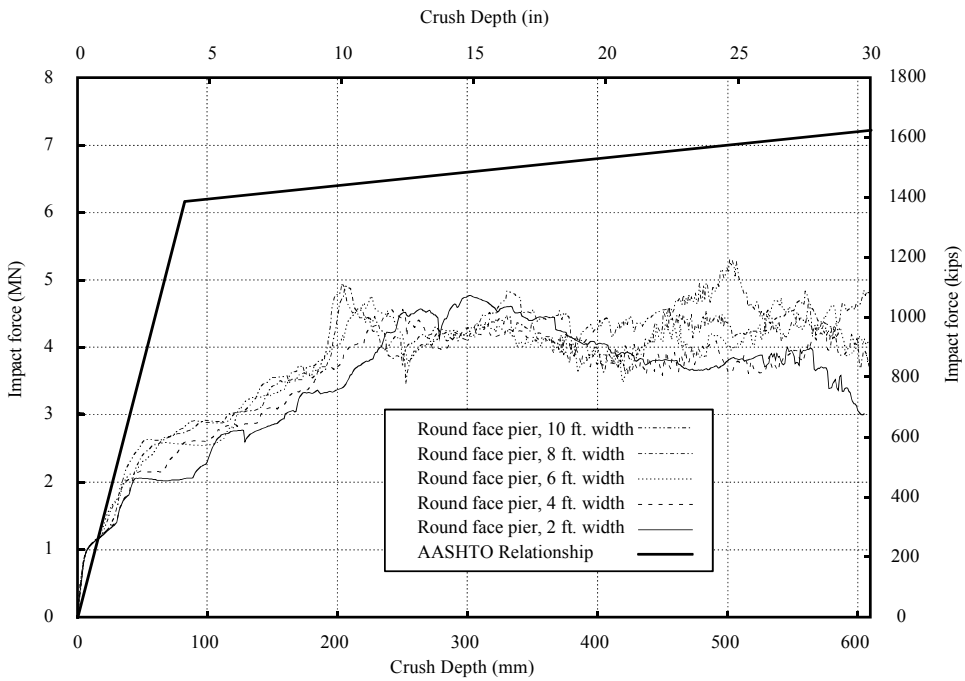

a)

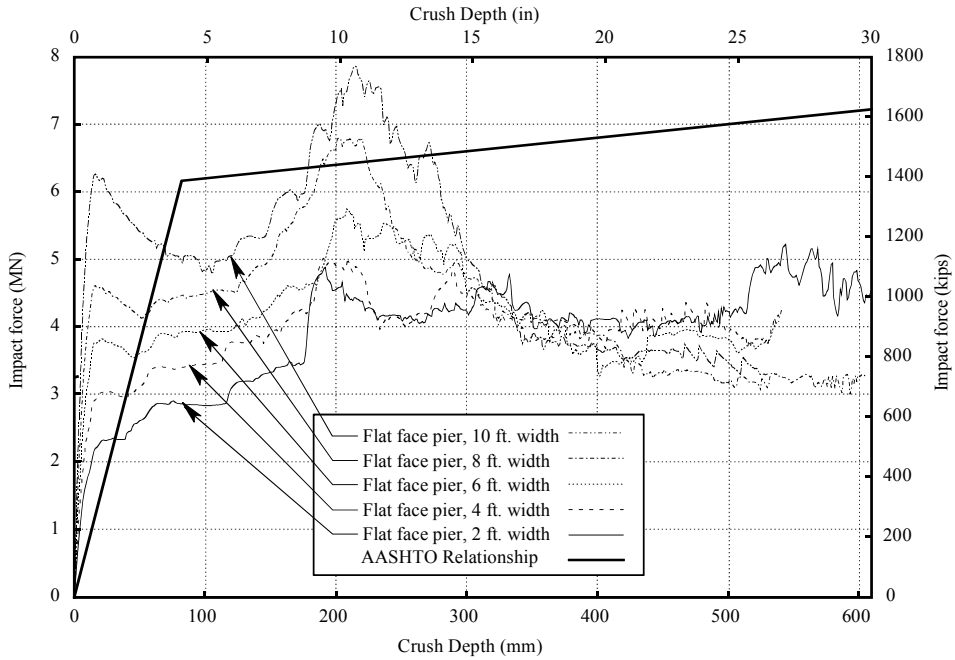

b)

Figure 3.6 Comparison of crush simulation data and AASHTO crush model

CHAPTER 4
NONLINEAR DYNAMIC COMPUTATIONAL PROCEDURE

4.1 Overview

The efficient analysis procedure documented here involves coupling a single degree of freedom (DOF) nonlinear barge model to a multi-DOF nonlinear dynamic pier analysis code. Dynamic barge and pier behavior are analyzed separately in distinct code modules that are then linked together (Figure 4.1) through a common contact-force (impact-force) to facilitate coupled barge-pier collision analysis. A primary advantage of this modular approach is that it encapsulates all aspects of barge behavior (e.g. characterization of crushing relationships) in a self-contained module that can be integrated into existing nonlinear dynamic pier analysis codes with relative ease. In this thesis, the single DOF barge module is integrated into the multi-DOF commercial pier analysis program FB-Pier [17,18]. Simple communication links permit continuous interchange of displacement and force data between the barge and pier modules. However, ensuring acceptable rates of convergence for two distinct but coupled modules, each representing the behavior of a nonlinear dynamic system, also necessitates the use of special convergence acceleration techniques as will be described later.

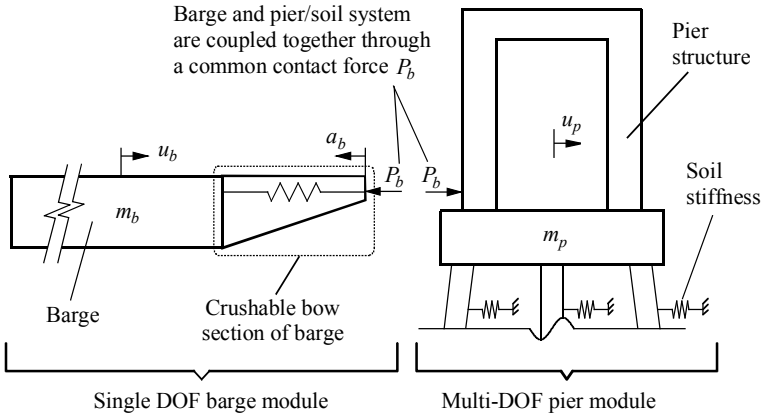

Figure 4.1 Barge and pier modeled as separate but coupled modules

4.2 Modeling Nonlinear Dynamic Barge Behavior

Due to the nature of barge impacts, analysis of such events requires both the nonlinear structural behavior (force-deformation response) and the inertial properties of the barge be modeled accurately. Inaccurate force-deformation relationships not only affect loads imparted to the structure, but also affect the dissipation of kinetic energy during impact. A substantial portion of the initial kinetic energy of the barge is dissipated through the deformation of the barge head log. This is especially true during high-energy impacts when the barge is expected to sustain large permanent deformations.

For the research done in this study, nonlinear structural behavior is modeled by force-deformation curves (the development of which was discussed in the previous chapter) that represent crushing of the barge bow. The entire mass of the barge is represented as an independent single degree of freedom (SDOF) mass. The barge SDOF mass representation is coupled with the pier model at the point of contact, through the contact force.

4.2.1 Force-Deformation Relationships

During barge collisions with bridge piers, the bow section of the barge will typically undergo permanent plastic deformation. However, depending on the impact speed, barge type, and pier flexibility, dynamic fluctuation may occur [19,20] that produces loading with plastic deformation (as discussed previously), unloading, and subsequent *reloading* of the bow. In the barge model proposed here, representation of this behavior is achieved by tracking the deformation state of the barge throughout the dynamic collision event. In Figure 4.2, the various stages of barge bow loading, unloading, and reloading are illustrated. Whenever the barge is in contact with the pier, the crush is computed as $a_b = \left(u_b - u_p\right)$, where u_b and u_p are the barge and pier displacements, respectively.

Upon contact with a bridge pier, the barge bow loads elastically until the crush depth (deformation level) a_b exceeds the yield value a_{by}. For crush depths $a_b > a_{by}$, plastic deformation of the bow is assumed to occur (Figure 4.2a). Continued loading generates additional plastic deformation as the plastic loading curve is followed. At some stage in the collision event, the contact force (P_b) between the barge and the pier may diminish (e.g., due to barge deceleration, or pier acceleration in response to impulsive loading). As this occurs, the crush depth a_b will drop (Figure 4.2b) rapidly from the maximum sustained level a_{bmax} to the residual plastic deformation level a_{bp} as the barge bow unloads. Once the condition $P_b = 0$ is reached, all elastic deformation ($a_{bmax} - a_{bp}$) will have been recovered. When $a_b < a_{bp}$ (Figure 4.2c), the barge is not

physically in contact with the pier and therefore $P_b = 0$. If reloading subsequently occurs (e.g., due to rebound of the pier once soil resistance has been mobilized), the unloading/reloading path will be followed back up to the loading curve (Figure 4.2d) and plastic deformation will once again initiate when a_b exceeds the previously achieved a_{bmax}.

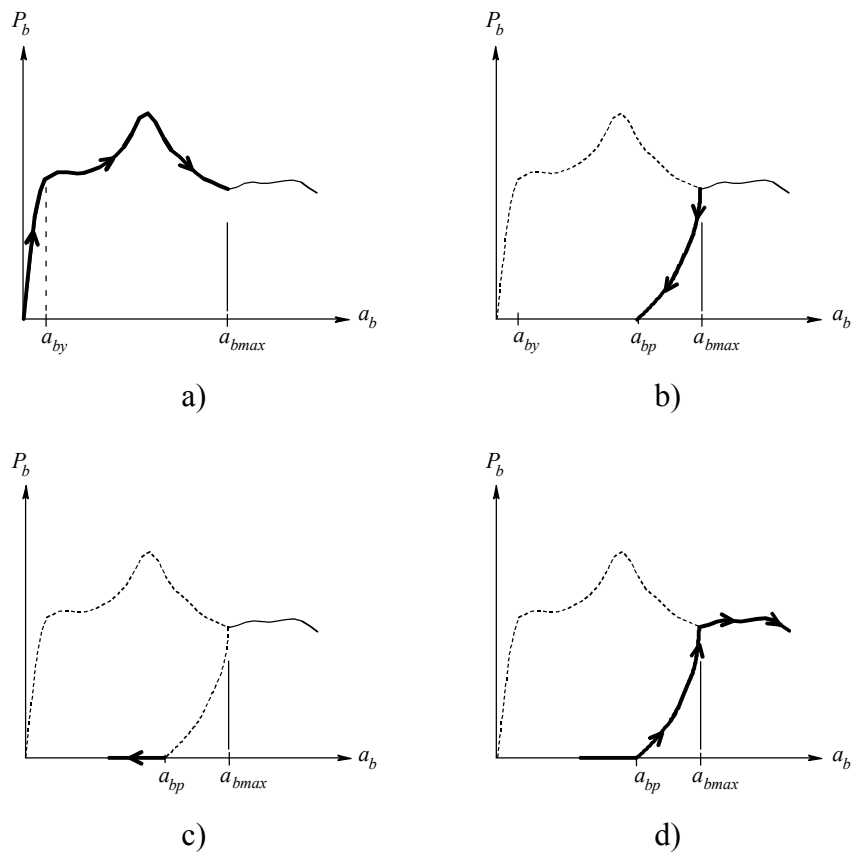

Figure 4.2 Stages of barge crush
a) Loading; b) Unloading; c) Barge not in contact with pier;
d) Reloading and continued plastic deformation

Algorithmically, the barge behavior illustrated in Figure 4.2 is modeled as a nonlinear compression-only (zero-tension) spring. Loading and unloading data for the spring are obtained from static finite element crush analyses conducted using a high-resolution model (>25,000 shell elements) of a barge [15]. Key to the concept of using

high resolution finite element analyses for the purpose of generating crush-curve data is the idea that such analyses are one-time events conducted in advance for a given barge type and pier shape/size. Once completed, results from these analyses can be stored in a database and subsequently retrieved for use in the SDOF barge model described here.

In Figure 4.3, loading curves generated in the manner described in the previous chapter are presented for a jumbo hopper barge being monotonically crushed (impacted) by circular and square piers 1.8 m (6 ft.) in width. Unloading curves are obtained similarly, with the sole difference being that *cyclic* crush analyses (Figure 4.4), rather than monotonic crush analyses, are required. As the name implies, cyclic crush analyses involve repeated cycles of loading and unloading. Forces P_b and crush deformations a_b are monitored throughout the analysis process. Each time a cycle of loading ends and unloading begins, the maximum sustained crush deformation a_{bmax} is recorded. Unloading from this stage down to the condition $P_b = 0$ then forms an unloading curve corresponding to the recorded value of a_{bmax}. After multiple cycles of loading and unloading, a collection of unloading/reloading curves is produced (Figure 4.5).

When such curves are used to model barge unloading behavior during a dynamic collision analysis, the deformation level a_{bmax} at which unloading begins will normally not correspond to one of the values recorded during the cyclic crush analysis. In such a situation, the unloading curves are scanned until two curves are located such that $a_{bmax(i)} \leq a_{bmax} \leq a_{bmax(i+1)}$. An intermediate unloading curve is then generated for deformation level a_{bmax} by linearly interpolating between the two bounding curves (Figure 4.6).

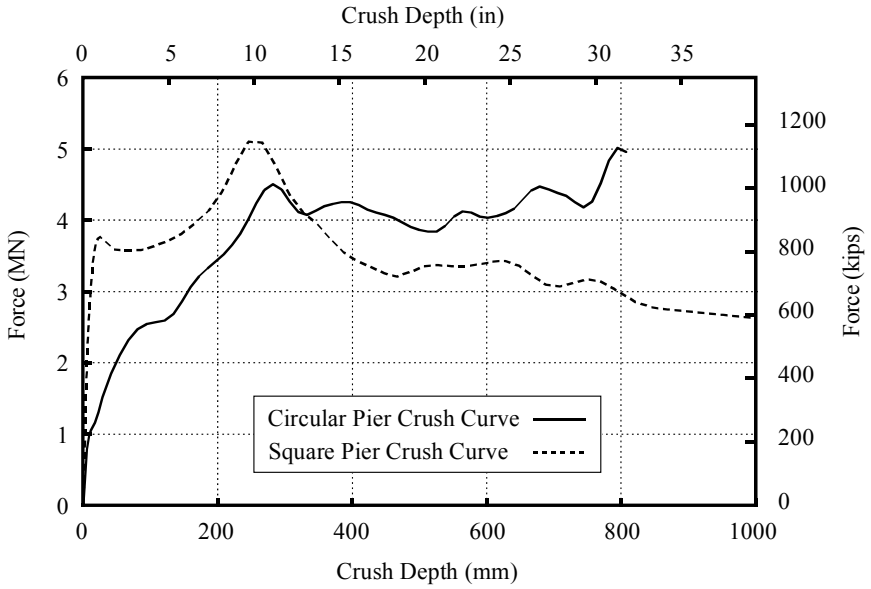

Figure 4.3 Barge force-deformation relationships obtained from high resolution static crush analyses

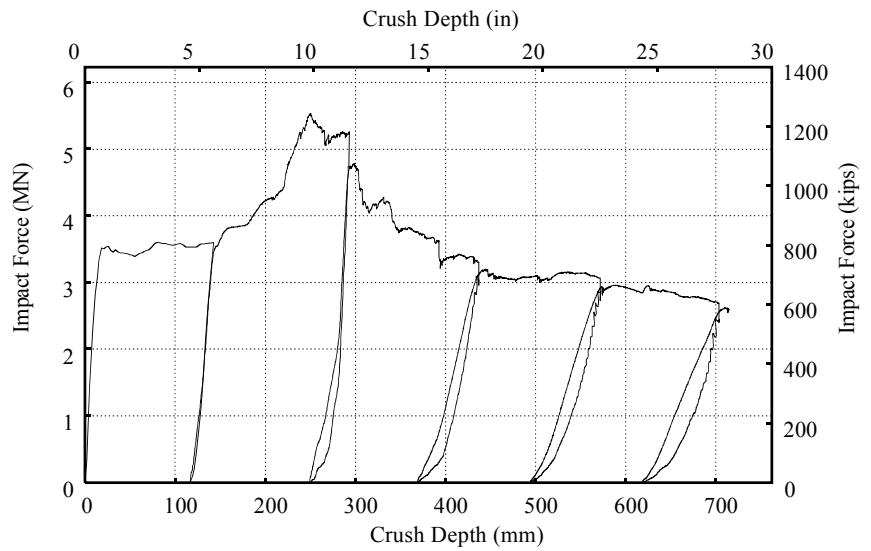

Figure 4.4 Barge unloading curves obtained from high resolution cyclic static crush analyses

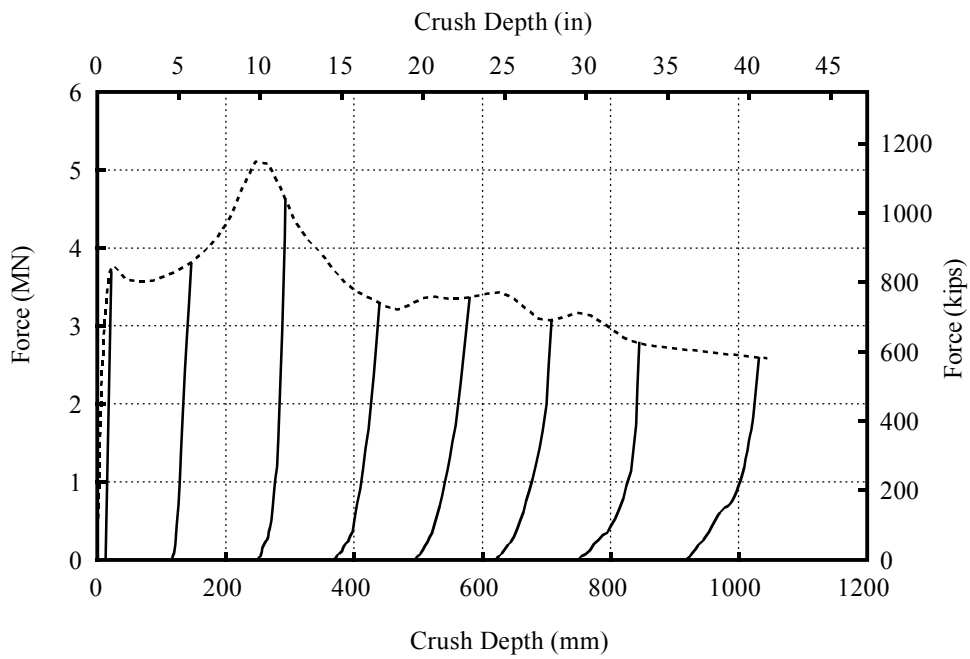

Figure 4.5 Unloading curves generated by cyclic high-resolution crush analysis

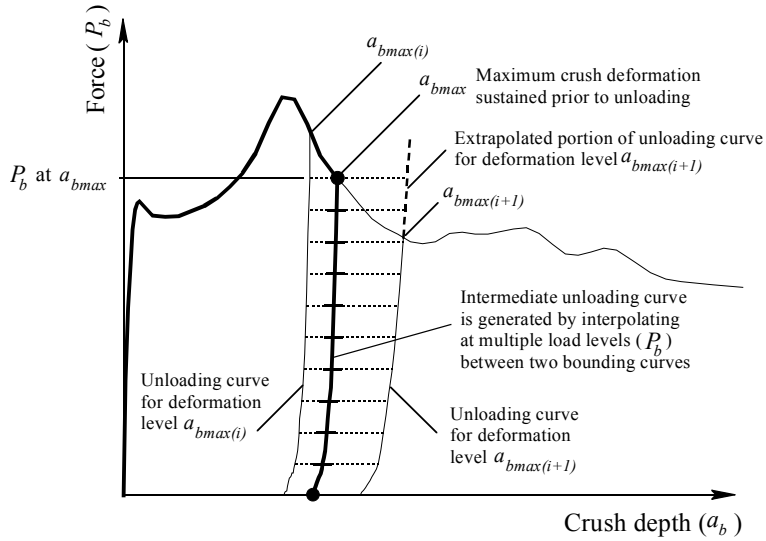

Figure 4.6 Generation of intermediate unloading curves by interpolation

4.2.2 Time Integration of Barge Equation of Motion

Since the process of crushing the barge is nonlinear, the only pragmatic procedure to time-integrate the barge equation of motion is through the use of numerical procedures. In this present study, any effects (such as viscous damping) of the water in which the barge is suspended are neglected as these effects are beyond the scope of the current research. However, energy dissipation as a result of inelastic deformation of the barge head log is accounted for in the current model. Recalling Figure 4.1, the equation of motion for the barge (single degree of freedom, SDOF) is written as :

$$m_b \ddot{u}_b = P_b \tag{4.1}$$

where m_b is the barge mass, $\ddot{u}_b$ is the barge acceleration (or deceleration), and P_b is the contact force acting between the barge and pier. Evaluating Eq. 4.1 at time t--with the assumption that the mass remains constant—we have

$$m_b \, {}^t\ddot{u}_b = {}^tP_b \tag{4.2}$$

where ${}^t\ddot{u}_b$ and ${}^tP_b$ are the barge acceleration and force at time t. The acceleration of the barge at time t is estimated using the central difference equation :

$${}^t\ddot{u}_b = \frac{1}{h^2}({}^{t+h}u_b - 2\,{}^tu_b + {}^{t-h}u_b) \tag{4.3}$$

where h is the time step size; and ${}^{t+h}u_b$, ${}^tu_b$, and ${}^{t-h}u_b$ are the barge displacements at times $t+h$, t, and $t-h$ respectively. Substituting Eq. 4.3 into Eq. 4.2 yields the explicit integration central difference method (CDM) dynamic update equation :

$${}^{t+h}u_b = -({}^tP_b\, h^2 / m_b) + 2\,{}^tu_b - {}^{t-h}u_b \tag{4.4}$$

which uses data at times t and $t-h$ to predict the displacement ${}^{t+h}u_b$ of the barge at time $t+h$. Using the force-deformation relationships described earlier, the force ${}^{t}P_b$ is computed.

4.2.3 Coupling Between Barge and Pier

The analytical coupling procedure presented here is based on earlier work conducted by Consolazio and Hendrix [19,21], but has been enhanced and expanded from the previous studies. Modifications to the procedure include improved characterization of barge crushing—most notably the unloading procedure—and the ability to incorporate oblique angle impact conditions.

As previously mentioned, the SDOF barge model is coupled to the pier-soil model through a shared contact force. For demonstrative purposes, the procedure outlined here is implemented in the FB-Pier substructure analysis program. The barge and the pier-soil models are handled as two independent modules (Figure 4.7). Essentially, the contact force between the barge and the pier is calculated by the barge module (Figure 4.8), using the generated force-deformation relationships, whereas the dynamic time-integration procedure is conducted within the pier-soil module.

Upon invocation of the barge module, an estimate of the contact force P_b is computed for the current time step. Calculation of this force is dependent upon the barge crush depth, calculated as $a_b = \max\left(\left(u_b - u_{pb}\right), a_{bp}\right)$, where u_{pb} is the component of pier motion in the direction of barge motion (Figure 4.9a), computed as $u_{pb} = u_{px}\cos(\theta_b) + u_{py}\sin(\theta_b)$. The pier-soil module has provided the most current updates of the x and y-displacements (u_{px} and u_{py} respectively) of the pier. The barge

module uses an iterative version of CDM to to satisfy the barge equation of motion [19,21]. Once the barge module has converged on a force value, this force is then resolved into x and y components (Figure 4.9b), calculated as $P_{bx} = P_b \cos(\theta_b)$ and $P_{by} = P_b \sin(\theta_b)$, and then applied to the pier-soil module as external loads. Upon convergence of the pier-soil module [22], the x and y components of the pier displacement are calculated and sent to the barge module. The barge module begins the convergence procedure over again until the contact force for the current cycle is calculated. The contact force for the current cycle is compared to the force from the previous cycle. If the difference calculated is sufficiently small, the barge/pier/soil system is considered to have achieved convergence, and the program repeats this procedure for the next time step.

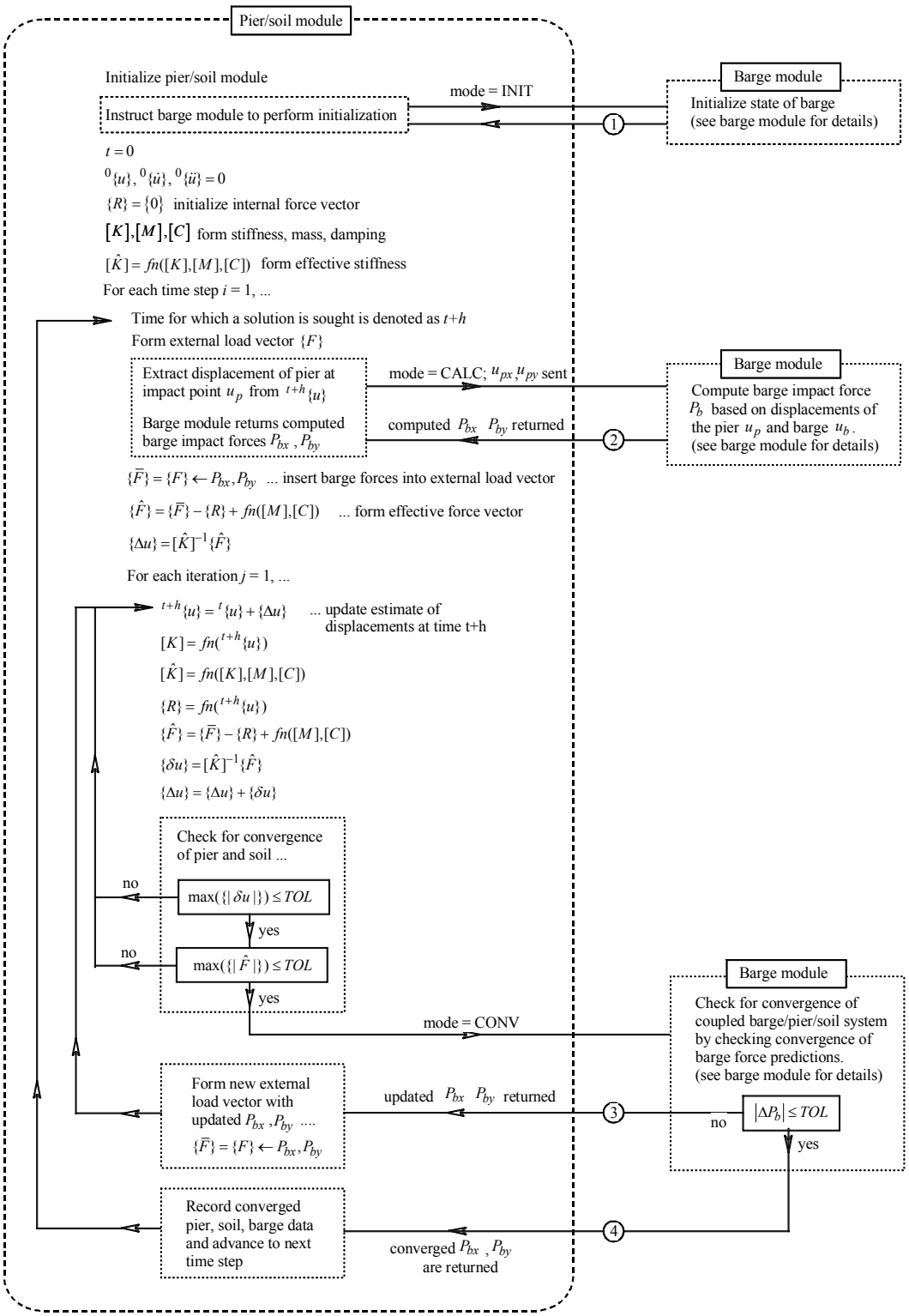

Figure 4.7 Flow-chart for nonlinear dynamic pier/soil control module (After [21] with modifications)

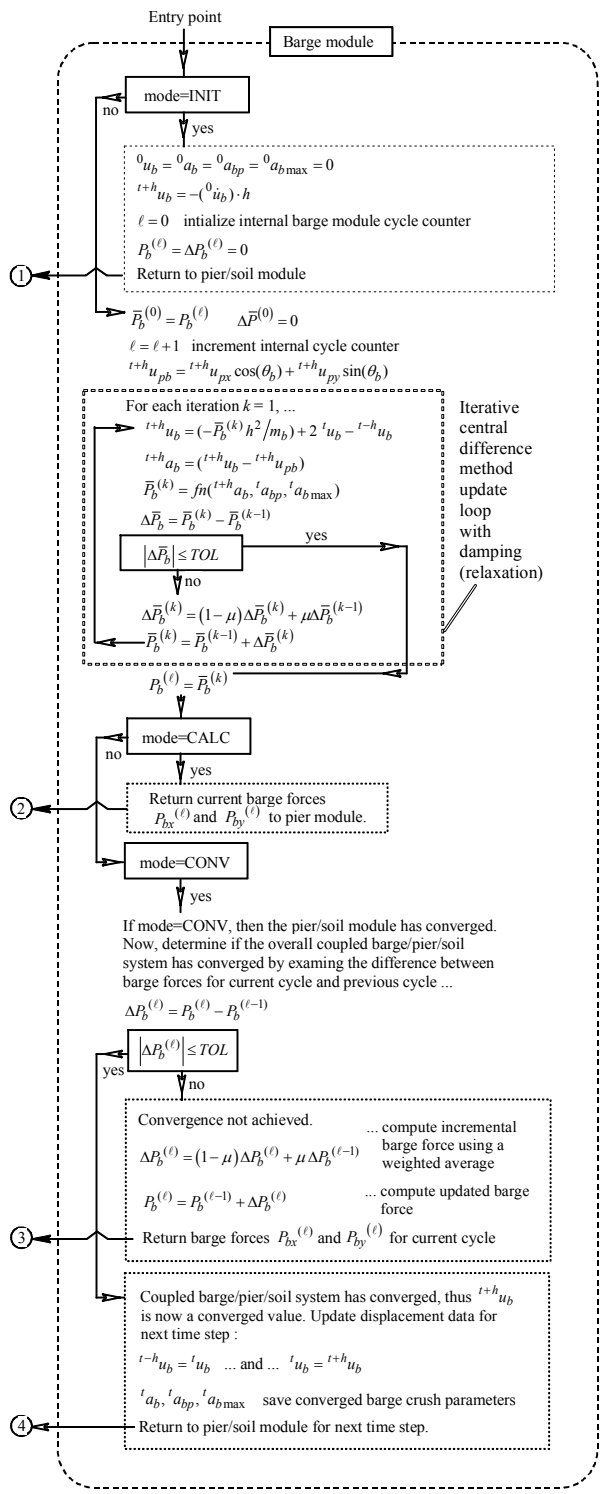

Figure 4.8 Flow-chart for nonlinear dynamic barge module (After [21] with modifications)

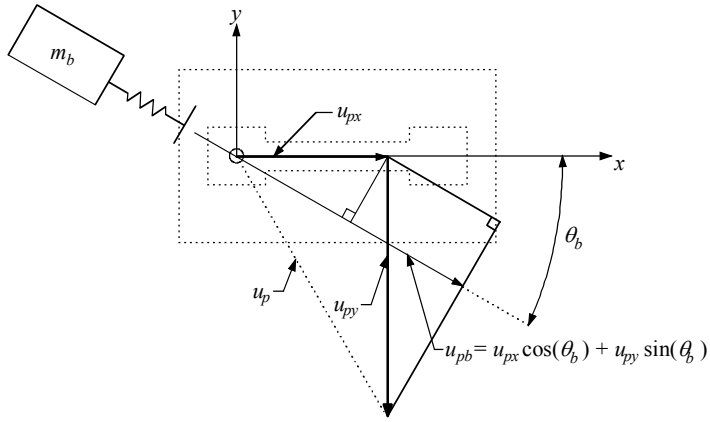

a)

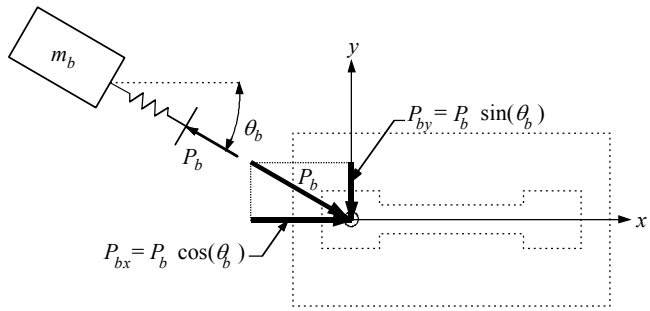

b)

Figure 4.9 Treatment of oblique collision conditions
a) Displacement transformation; b) Force transformation

CHAPTER 5
IMPACT ANALYSIS RESULTS

5.1 Introduction

For purposes of validating and demonstrating the proposed collision analysis procedure, two bridge piers (Figure 5.1) will be considered here. Structural data and soil information for the two piers were obtained from construction drawings and soil boring logs for two bridges that each have (at some point in time) spanned across Apalachicola Bay near St. George Island, Florida. Pier-A is a channel pier of a bridge that was constructed in the 1960s and which has now been replaced. Pier-B is a channel pier of the replacement structure currently in place. Given that Pier-B has been designed to meet present day design standards for vessel-collision resistance, it possess significantly more lateral load carrying capacity. The two piers represent a wide variety of bridge piers currently in service: Pier-A being representative of older structures still in service; and Pier-B being representative of newly constructed bridges.

The steel H-piles supporting pier-A were given an elastic perfectly plastic steel material model with a yield stress of 413.7 Mpa (60 ksi) and a modulus of elasticity of 200.0 Gpa (29,000ksi). Concrete properties for each peir are presented in Table 5.1.

Table 5.1 Pier Concrete Properties

	28-day compressive strength MPa (ksi)	Modulus of Elasticity GPa (ksi)
Pier-A	41.37 (6)	30.44 (4415)
Pier-B	37.92 (5.5)	29.14 (4227)
Pier-B piles	48.26 (7)	32.88 (4769)

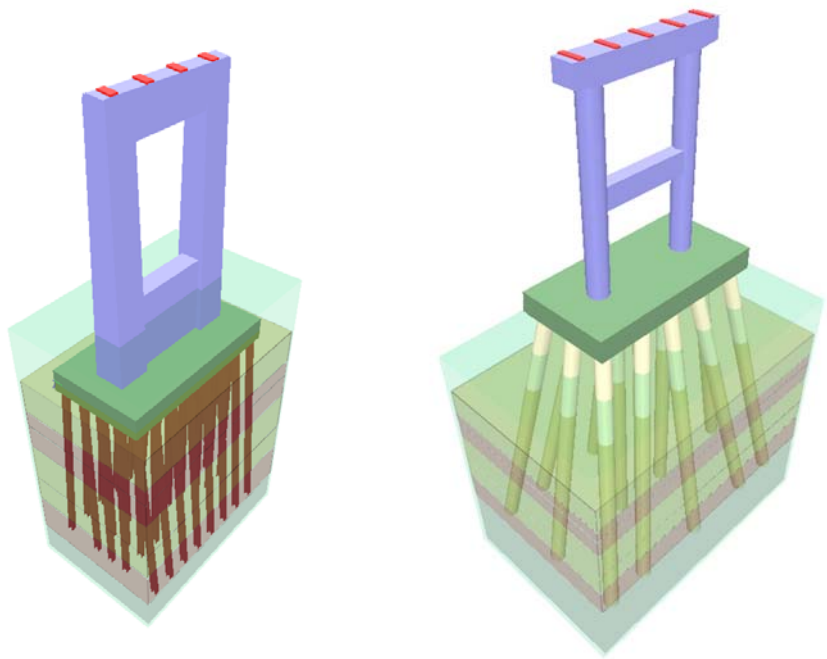

a) b)

Figure 5.1 Structural pier configurations analyzed (not to relative scale).
a) Pier-A (constructed in 1960s; b) Pier-B (constructed in 2000s)

5.2 Validation Case

To assess the accuracy of the proposed analysis procedure, a validation case is now considered. High-resolution models of both Pier-A and a jumbo hopper barge (Figure 5.2) were previously generated [20] and analyzed using the contact-impact finite element code LS-DYNA [13]. In addition, a corresponding model for the same pier was also generated (Figure 5.1a) for analysis using the barge-modified FB-Pier code outlined in Figure 4.7.

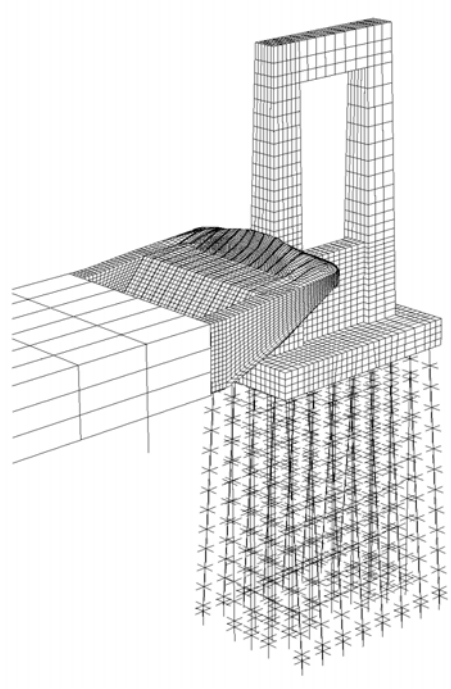

Figure 5.2 High resolution model used for validation

The primary difference between the LS-DYNA and FB-Pier analysis models lies in the complexity of the barge model. In the high-resolution LS-DYNA model, the bow area (impact zone) of the barge is modeled using more than 25,000 shell elements that, through the use of nonlinear material models, are capable of sustaining permanent deformation. The remainder of the barge is modeled using 8-node solid brick elements to yield correct inertial properties. In the barge-modified FB-Pier model, the hopper barge is reduced to a single point mass and a single nonlinear spring. Loading and unloading curves (i.e., nonlinear spring data) specified for the barge are those previously illustrated in Figure 4.5 for a hopper barge being impacted by a 1.8 m (6ft.) wide square pier.

Barge collision analyses are run using both techniques for a head-on condition (impact angle θ_b=0) with a single fully loaded hopper barge (total weight, 16.9 MN (1900 tons)), traveling at an impact speed of 2.05 m/s (4 knots). Comparisons of analysis

results obtained from the two methods are presented in Figure 5.3. With regard to the dynamic impact forces predicted by the two methods (Figure 5.3a), good agreement is observed in force magnitude and temporal-variation. The one notable exception (at approximately $t = 1.2$ sec) is due to a premature prediction of unloading in the simplified barge model. This is evident in Figure 5.3b where initial unloading occurs at a lesser deformation level in the simplified model. However, considering that the areas under the load-deformation curves in Figure 5.3b are quite similar, it is also observed that predictions of energy dissipation associated with barge crush are quite similar. Finally, pier displacement time-histories (Figure 5.3c) indicate closely matched predictions of pier motion, and therefore pile shears and moments.

5.3 Demonstration Applications

Three brief case studies are now presented to demonstrate how the proposed collision analysis procedure may be used to efficiently evaluate pier response under a variety of different conditions. All impact conditions presented in this section involve fully loaded hopper barges striking bridge piers. For the first two cases the velocity of the barge upon impact is 1.80 m/s (3.5 knots). However, for the last case study, the barge velocity was decreased to 1.29 m/s (2.5 knots).

In Case Study 1 (Figure 5.4), the effects of pier stiffness and column cross-sectional shape are evaluated. Barge collisions are analyzed for Pier-A with square columns, Pier-B with square columns, and Pier-B with circular columns. Barge crush curves (loading curves) for the square and circular columns used in these analyses are illustrated in Fig. 3. By comparing the two square column analyses, the effect of pier stiffness may be isolated. Similarly, by comparing the two Pier-B analyses, the effect of

column shape may be isolated. Examining Figure 5.4c, it is clear that the more flexible, older, less impact resistant Pier-A sustains significantly more pier motion than does the stiffer Pier-B. However, it is noteworthy that the force histories and force-deformation loops (energy dissipation indicators) are quite similar. From the results shown, it is evident that if a pier possesses sufficient stiffness to initiate plastic barge deformation, the loads generated after initial yielding will not vary widely.

In Case Study 2 (Figure 5.5), the effects of oblique collision angles are evaluated by conducting impact analyses at angles $\theta_b = 0$, 15, 30, 45, and 60 degrees. Pier-B was chosen for these simulations because the columns of this pier are circular in shape (Figure 5.1b), and therefore the barge crush curve is independent of impact angle θ_b. The force results obtained indicate that the pier has sufficient stiffness in all directions to initiate and propagate plastic barge crushing, thus producing nearly identical load histories. Pier motions in the x and y directions demonstrate that the proposed analysis procedure is capable of predicting biaxial pier response parameters (e.g. displacements, pile moments, shears, etc.) under oblique impact conditions.

In Case Study 3 (Figure 5.6), the proposed analysis procedure is used to analyze the response of Pier-B when struck by a single fully loaded hopper barge, and when struck by a small flotilla of two in-line fully loaded hopper barges. In the latter case, the mass of the SDOF barge model is doubled to reflect the presence of the second barge. As the kinetic energy of the barge flotilla is doubled by doubling the mass, the energy *dissipated* through plastic barge deformation (approximately equal to the area under the curve in Figure 5.6b) is also observed to approximately double. However, both of the indicators of structural demand, specifically the collision forces and the pier

displacements, are virtually unaltered in magnitude as a result of the doubled kinetic impact energy. Current vessel-collision design guidelines [7] stipulate that the equivalent static impact forces used for design purposes increase continuously with increasing kinetic energy (and therefore increasing flotilla mass). Results obtained from this case study indicate that such continuous increases may not be appropriate.

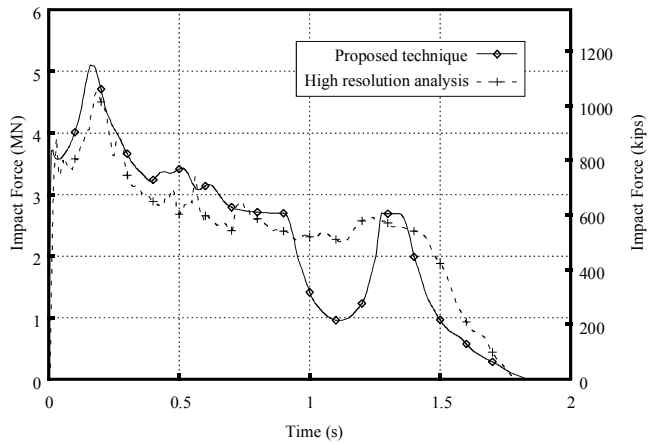

a)

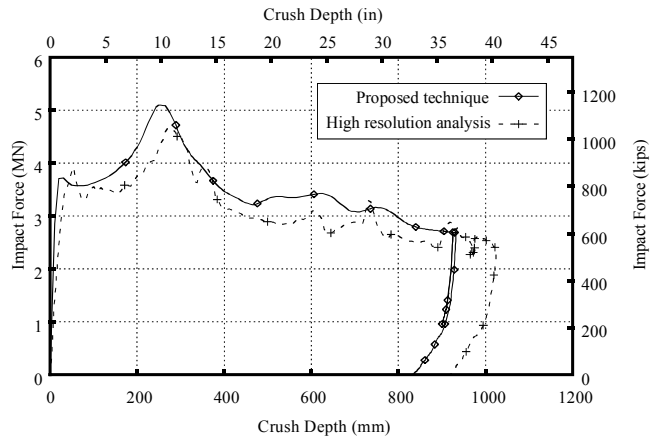

b)

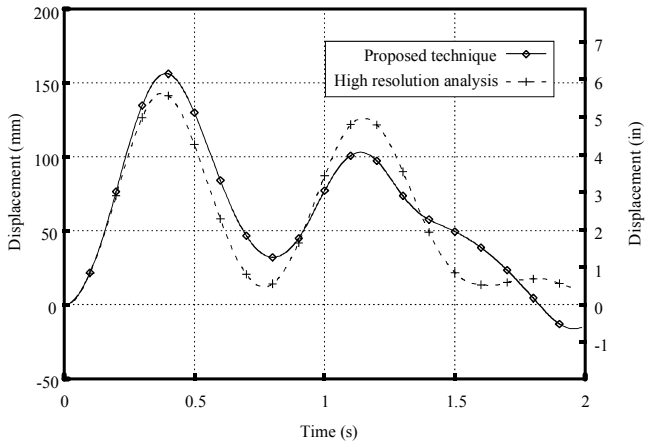

c)

Figure 5.3 Comparison of proposed analysis technique and high resolution simulation
a) Impact force; b) Barge force-deformation; c)Pier displacement

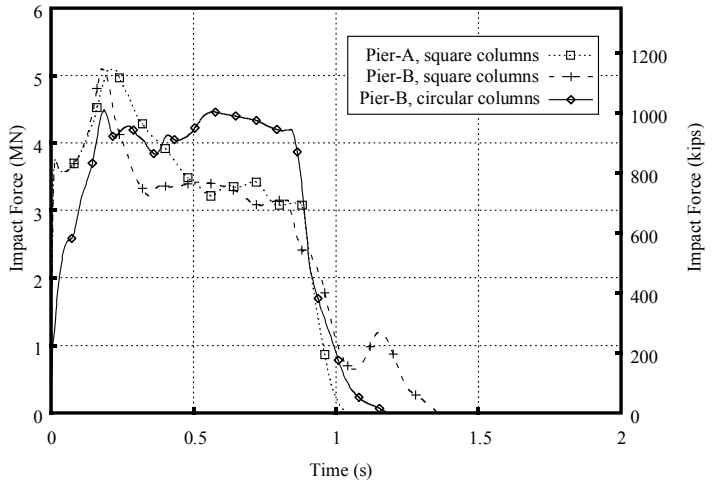

a)

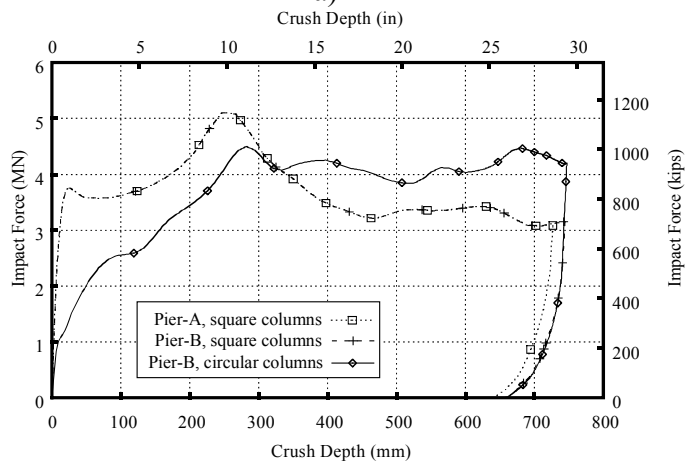

b)

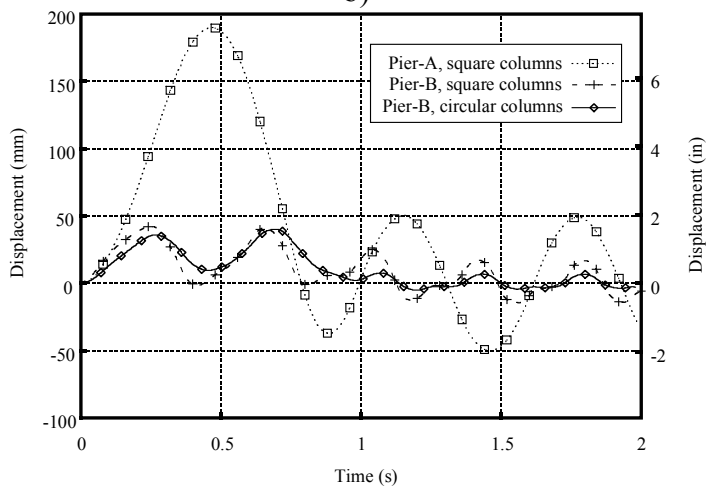

c)

Figure 5.4 Effect of pier stiffness and pier-column geometry
a) Impact force; b) Barge force-deformation; c)Pier displacement

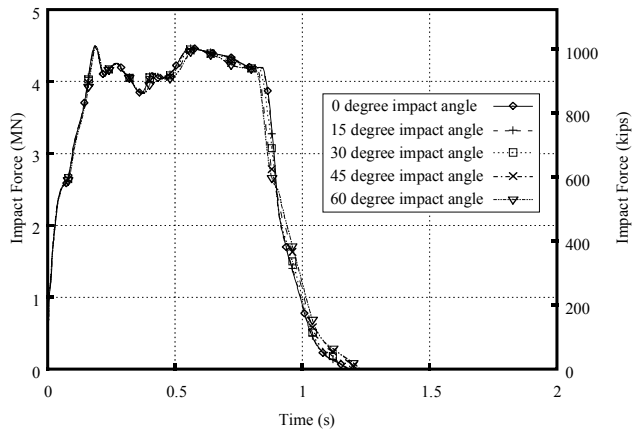

a)

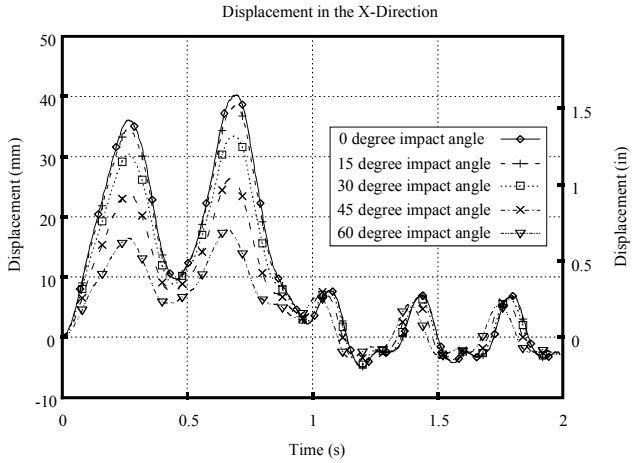

b)

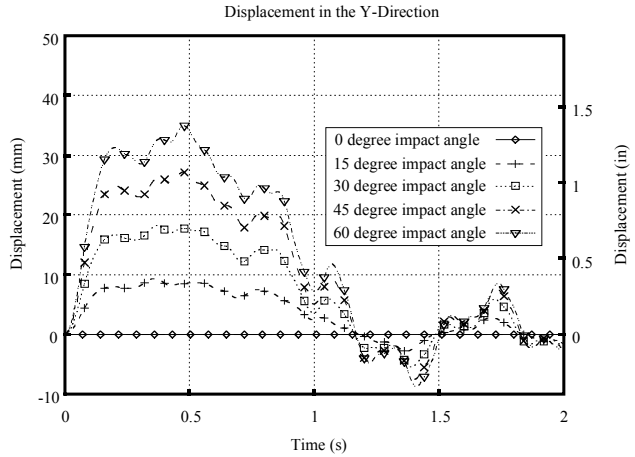

c)

Figure 5.5 Effect of oblique collision angle
a) Impact force; b) Longitudinal (*x*) pier displacement; c) Lateral (*y*) pier displacement

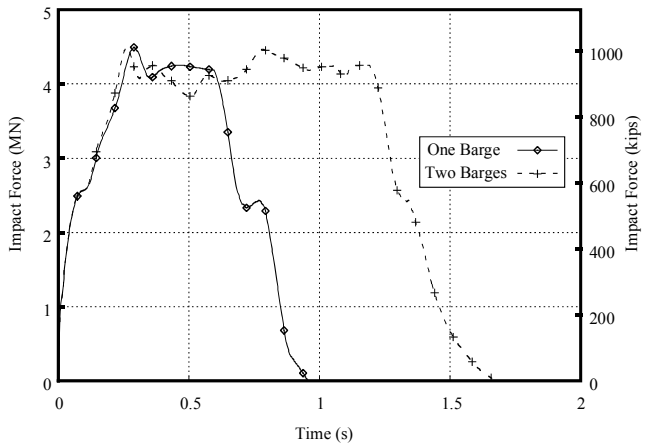

a)

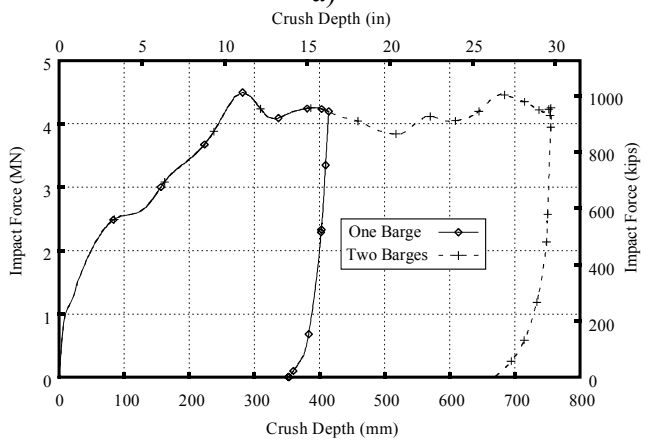

b)

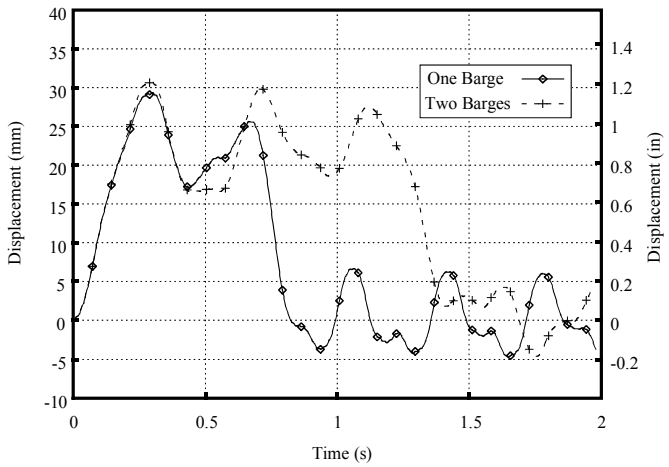

c)

Figure 5.6 Effect of barge flotilla size
a) Impact force; b) Barge force-deformation; c)Pier displacement

CHAPTER 6
CONCLUSIONS AND RECOMMENDATIONS FOR FUTURE RESEARCH

A numerically efficient barge collision analysis procedure has been presented that involves coupling nonlinear dynamic single degree of freedom (SDOF) barge models to existing nonlinear dynamic multi-degree of freedom (MDOF) pier analysis codes. Methods of modeling barge crushing stiffness, plastic crushing deformation, unloading, and dynamic behavior have been presented. A strategy for coupling SDOF barge models and MDOF pier/soil models together through a shared impact force parameter has been described, implemented, validated, and demonstrated. The proposed method is modular and can easily incorporate new barge types. The modular approach proposed requires minimal effort to implement the barge module into existing pier analysis codes. Similarly, the fact that barge loading and unloading characteristics are modeled with user defined curves means that new crush models corresponding to other types of vessels may be easily integrated. Finally, the influence of parameters such as barge type and mass, impact speed and angle, and pier configuration can be efficiently evaluated using the proposed nonlinear dynamic collision analysis method.

6.1 Conclusions

AASHTO provisions assume that the peak impact load occurs at the maximum crush depth for the vessel. However, results from analyses conducted in this study have shown that at large deformations the impact force can be greater than the force at lower deformation levels. Results from square impactor crush analyses exhibit this behavior,

whereas results from circular impactor crush analyses appear to have force values that increase monotonically with crush depth. Thus, static crush results presented in this thesis indicate that, for flat-faced piers, the existing procedures should be reexamined since the peak impact force is not necessarily correlated to maximum crush depth.

Furthermore, it should be noted that, for square impactors, as the width of the impact face increases, so does the magnitude of the impact force. On the contrary, for the circular impactors, the diameter of the pier has negligible effect on the magnitude of the force.

Conclusions drawn from several brief case studies presented here offer additional insight into barge collision loading conditions. In cases where a pier has sufficient stiffness to initiate plastic barge deformation during impact, pier column shape and overall pier stiffness have been found to have only marginal influence on the sustained impact forces generated. Separate results obtained from a single barge collision analysis and a two-barge flotilla collision analysis suggest that increasing the total mass of a barge flotilla may not necessarily impose additional structural demand on the pier. This is apparently due to the fact that the additional kinetic impact energy is dissipated through increased plastic barge deformation.

6.2 Recommendations for Future Research

In this study, the effects of multiple barges in a flotilla have been approximated by increasing the mass of the SDOF barge model. However, a single barge with doubled mass may not behave the same way as two linked barges. Therefore, as a suggestion for future research, one could implement a MDOF barge flotilla model in which each barge

is modeled as a SDOF object. Furthermore, nonlinear springs between barges can be used to model the forces between them during impact.

In the AASHTO design provisions, the equation for the barge kinetic energy includes a hydrodynamic mass coefficient. Consequently, future research efforts should incorporate the mass of water traveling with the barge during impact and any associated viscous drag effects. Such enhancements might affect the magnitude and duration of the impact force imparted to the pier.

In most vessel-structure impact scenarios, an in-service structure is impacted by the vessel. Thus, the bridge superstructure can play an important role in redistributing loads from the impact pier to adjacent piers. Parametric studies should be conducted in the future to quantify the effects of superstructure mass and stiffness, stiffness and mass of not only the impact piers, but also adjacent piers.

Finally, when a pier is impacted by a vessel, a substantial portion of the load is transmitted through the foundation into the soil. Current models include the force-deformation characteristics of the soil. As the soil deforms however, an associated mass of soil is mobilized that increases the inertial resistance of the pier-soil unit. Furthermore, rate of loading also affects the behavior of the pier-soil unit. In future studies, the inclusion of both soil mass and load-rate effects, and their affect on the response of the pier to impact loading should be given additional attention.

REFERENCES

1 Knott, M. and Prucz, Z. Vessel Collision Design of Bridges. In *Bridge Engineering Handbook*. Edited by Chen, W.F., and Duan, L., CRC Press LLC, Boca Raton, FL. pp 60-1 – 60-18, 2000.

2 Meir-Dornberg, KE. "Ship Collisions, Safety Zones, and Loading Assumptions for Structures in Inland Waterways." VDI-Berichte. No 496, pp.1-9, 1983.

3 Arroyo, J.R., Ebeling, R. M., and Barker, B.C. "Analysis of Impact Loads from Full-Scale, Low-Velocity, Controlled Barge Impact Experiments." ERDC/ITL TR-03-3, Army Corps of Engineers. 1998

4 Jagannathan, S. and Gray, D. L. "An Analytical Model for Barge Collisions with Rigid Structures." 14th International Conference on Offshore Mechanics and Arctic Engineering. Copenhagen, Denmark. June 18-22, 1995.

5 Minorsky, V.U. "An Analysis of Ship Collisons with Reference to Protection of Nuclear Power Plants." *Journal of Ship Research*. Vol 3, No 2, pp.1-4, 1959.

6 Woisin, G. "The Collision Tests of the GKSS." *Jahrbuch der Schiffbautechnischen Gesellschaft.* No 70, 465-487, 1976.

7 American Association of State Highway and Transportation Officials (AASHTO). *Guide Specification and Commentary for Vessel Collision Design of. Highway Bridges*. American Association of State Highway Transportation Officials, Washington, DC, 1991.

8 Kitamura, O. "FEM Approach to the Simulation of Collision and Grounding Damage." *Marine Structures.* Vol 15, No 4-5, pp. 403-428, 2002.

9 Lehmann, E. and Peschmann, J. "Energy Absorption by the Steel Structure of Ships in the Event of Collisions." *Marine Structures.* Vol 15, No 4-5, pp. 429-441, 2002.

10 Chen, D. "Simplified Ship Collision Model." Master's Thesis, Department of Ocean Engineering, Virginia Polytechnic Institute and State University, Blacksburg, Virginia, 2000 (Advisor: A.J. Brown).

11 Frieze, P. A. and Smedley, P. A. "Ship Bow Damage During Impacts with Ships and Bridge Piers." International Conference on Collision and Grounding of Ships. Copenhagen, Denmark. 2001.

12 American Association of State Highway and Transportation Officials (AASHTO). *LRFD Bridge Design Specifications and Commentary*. American Association of State Highway and Transportation Officials, Washington, DC , 1994.

13 Livermore Software Technology Corporation (LSTC). *LS-DYNA Theoretical Manual*. Livermore, CA, 1998.

14 Consolazio, G.R., Cook, R.A., Lehr, G.B,, and Bollmann, H.T. "Barge Impact Testing of the St. George Island Causeway Bridge Phase I: Feasibility Study." Structures Research Report No. 783, Engineering and Industrial Experiment Station, University of Florida, Gainesville, Florida, January 2002.

15 Consolazio, G.R., Cook, R.A., Biggs, A.E., Cowan, D.R., and Bollmann, H.T. "Barge Impact Testing of the St. George Island Causeway Bridge Phase II: Design of Instrumentation Systems." Structures Research Report No. 883, Engineering and Industrial Experiment Station, University of Florida, Gainesville, Florida, April 2003.

16 Consolazio, G.R., Cowan, D.R. "Nonlinear Analysis of Barge Crush Behavior and its Relationship to Impact Resistant Bridge Design." *Computers and Structures*. Vol 81, No 8-11, pp. 547-557, 2003.

17 Florida Bridge Software Institute. *FB-PIER Users Manual*. University of Florida, Department of Civil & Coastal Engineering, 2000.

18 Brown, D.A., O'Neill, M.W., Hoit, M., McVay, M., El Naggar, M.H., and Chakraborty, S. "Static and Dynamic Lateral Loading of Pile Groups." Report 461. NCHRP, Transportation Research Board. 2001.

19 Consolazio, G.R., Hendrix, J.L., McVay, M.C., Williams, M.E., and Bollmann, H.T. "Prediction of Pier Response to Barge Impacts Using Design-Oriented Dynamic Finite Element Analysis." *Journal of the Transportation Research Board*. Washington, D.C. (In Press).

20 Consolazio, G.R., Lehr, G.B., and McVay, M.C. "Dynamic Finite Element Analysis of Vessel-Pier-Soil Interaction During Barge Impact Events." *Journal of the Transportation Research Board*. No. 1849, Washington, D.C., pp. 81-90, 2004.

21 Hendrix, J.L. "Dynamic Analysis Techniques for Quantifying Bridge Pier Response to Barge Impact Loads." Masters Thesis, Department of Civil and Coastal Engineering, University of Florida, Gainesville, Florida, 2003 (Advisor: G.R. Consolazio).

22 Fernandez, C., Jr. "Nonlinear Dynamic Analysis of Bridge Piers." Ph.D. Dissertation, University of Florida, Department of Civil Engineering, University of Florida, Gainesville, Florida, 1999.

BIOGRAPHICAL SKETCH

The author was born in Akron, Ohio, on January 14, 1979. He began attending the University of Florida in January 1998. After obtaining his Bachelor of Science in Civil Engineering from the University of Florida in December of 2002, he began graduate school at the University of Florida in the College of Engineering. The author plans to receive his Master of Engineering degree in the August of 2004. Upon graduation, the author plans continue his education at the University of Florida seeking the degree of Doctor of Philosophy with a specialization in structural engineering.